Osteoblastic differentiation of periodontal ligament stem cells on non-stoichiometric calcium phosphate and titanium surfaces

Winning, L., Robinson, L., Boyd, A. R., El Karim, I. A., Lundy, F. T., & Meenan, BJ. (2017). Osteoblastic differentiation of periodontal ligament stem cells on non-stoichiometric calcium phosphate and titanium surfaces. *Journal of Biomedical Materials Research: Part A*, *105*(6), 1692-1702. https://doi.org/10.1002/jbm.a.36044

Link to publication record in Ulster University Research Portal

Published in:
Journal of Biomedical Materials Research: Part A

Publication Status:
Published (in print/issue): 01/06/2017

DOI:
10.1002/jbm.a.36044

Document Version
Author Accepted version

General rights
Copyright for the publications made accessible via Ulster University's Research Portal is retained by the author(s) and / or other copyright owners and it is a condition of accessing these publications that users recognise and abide by the legal requirements associated with these rights.

Take down policy
The Research Portal is Ulster University's institutional repository that provides access to Ulster's research outputs. Every effort has been made to ensure that content in the Research Portal does not infringe any person's rights, or applicable UK laws. If you discover content in the Research Portal that you believe breaches copyright or violates any law, please contact pure-support@ulster.ac.uk.

Download date: 05/05/2023

Society For Biomaterials

Osteoblastic differentiation of periodontal ligament stem cells on non-stoichiometric calcium phosphate and titanium surfaces

Lewis Winning,[1] Leanne Robinson,[2] Adrian R. Boyd,[2] Ikhlas A. El Karim,[1] Fionnuala T. Lundy,[1] Brian J. Meenan[2]

[1]Centre for Experimental Medicine, The Wellcome-Wolfson Institute for Experimental Medicine, School of Medicine, Dentistry and Biomedical Sciences, Queen's University Belfast, 97 Lisburn Road, Belfast, Northern Ireland, BT9 7BL, United Kingdom
[2]Nanotechnology and Integrated Bioengineering Centre (NIBEC), School of Engineering, Ulster University, Shore Road, Newtownabbey, Co. Antrim, Northern Ireland BT37 0QB, United Kingdom

Received 4 August 2016; revised 27 January 2017; accepted 16 February 2017
Published online 00 Month 2017 in Wiley Online Library (wileyonlinelibrary.com). DOI: 10.1002/jbm.a.36044

Abstract: Bioactive materials offer particular clinical benefits in the field of dental implantology, where differentiation of stem cells towards an osteoblastic lineage is required for osseointegration and appropriate function of implants *in vivo*. The aim of this study was to evaluate the osteoblastic response of Stro-1 +ve periodontal ligament stem cells (PDLSCs) to three well-characterized biomaterial surfaces: an abraded titanium surface (cpTi) control; a polycrystalline titanium surface, with both micro and nanotopography produced by radio frequency magnetron sputtering (TiTi); and the same surface incorporating a sputter deposited calcium phosphate coating (CaP-TiTi). The CaP-TiTi surfaces were nonstoichiometric, carbonated, and calcium rich with a Ca/P ratio of 1.74. PDLSCs were grown on each surface in the *absence* of supplementary osteogneic-inducing agents. Osteoblastic responses were assessed for up to 21 days in culture by measuring gene expression using real time q-PCR and via assessment of intracellular alkaline phosphatase (ALP) activity. Gene expression analysis for the CaP-TiTi surfaces showed a significant late stage up-regulation of Secreted Phosphoprotein 1. Additionally, there was a significant up-regulation of the Wnt signaling genes β-catenin and Wnt Family Member 5 A on days 14 and 21, respectively for the CaP-TiTi surface. A significant increase in intracellular ALP at day 21 for the CaP-TiTi surface was also observed. These data suggest that the CaP-TiTi surfaces provide the bioactive conditions required for direct osteoblastic differentiation of PDLSCs. © 2017 Wiley Periodicals, Inc. J Biomed Mater Res Part A: 00A:000–000, 2017.

Key Words: periodontal ligament stem cells, radio frequency magnetron sputtering, hydroxyapatite, osteoblastic differentiation, dental implants

How to cite this article: Winning L, Robinson L, Boyd AR, El Karim IA, Lundy FT, Meenan BJ. 2017. Osteoblastic differentiation of periodontal ligament stem cells on non-stoichiometric calcium phosphate and titanium surfaces. J Biomed Mater Res Part A 2017:00A:000–000.

INTRODUCTION

Mesenchymal stem cells (MSCs) are recognized as offering much promise in the areas of tissue engineering and regenerative medicine due to their ability to be differentiated to specific tissue forming cell types. Intense research effort has been directed toward examining bone marrow mesenchymal stem cells (BMMSCs) for applications in bone-tissue engineering.[1,2] By contrast, periodontal ligament stem cells (PDLSCs) are a relatively more recently described population of MSCs and have been shown to be both highly proliferative and multipotent.[3] PDLSCs also represent a promising source of stem cells owing to the relative ease in obtaining them compared with bone marrow harvesting. Within the field of dental implantology, PDLSCs have the potential to perform an important role during the osseointegration of devices when placed into fresh extraction sites (that is, "immediate" implant procedures). In addition, they also represent a source of stem cells for regenerative medicine applications, that could be applied around dental implants in areas where there is initially insufficient bone. Initial investigations have shown the potential of utilising PDLSCs to assess osteoblastic differentiation on various titanium surfaces.[4−7] However, their behavior in contact with bioactive materials such as hydroxyapatite (HA) and associated calcium phosphate (CaP) systems is less well understood.

In general, *in vitro* investigations examining the osteoblastic response of MSCs from various sources use an "osteogenic culture media" with chemical additives such as β-glycerolphosphate employed as supplements to promote biochemically initiated osteoblastic differentiation. There is inherent ambiguity in such models as the associated osteoblastic phenotype that develops is

Additional Supporting Information may be found in the online version of this article.
Correspondence to: F. T. Lundy; e-mail: f.lundy@qub.ac.uk
Contract grant sponsor: Department of Employment and Learning (Northern Ireland) and Northern Ireland Medical and Dental Training Agency (NIMDTA)

© 2017 WILEY PERIODICALS, INC.

not attributable to cell-substrate and/or cell-cell processes that normally regulate differentiation. Biomaterial surface-mediated events have previously been shown to directly trigger the commitment of undifferentiated cells toward an osteoprogenitor lineage and have been developed to offer an alternative starting point for osteogenesis.[8] Therefore, experimental models where surfaces that possess specific physical and chemical properties that can induce the osteoblastic differentiation of MSCs without the need for chemical supplementation in culture media are of increasing importance.

In this regard, specific forms of nanotopography created on titanium surfaces have been shown to induce direct osteoblastic differentiation in BMMSCs.[9] Furthermore, augmentation of such nanotopography with a bioactive chemistry, specifically that provided by HA and other CaP systems, has been shown to provide significant benefits in terms of enhanced osteoblastic differentiation.[10,11] HA has the potential to induce both osteoconductive, and osteoinductive cell responses and therefore represents a well-established platform to deliver the appropriate surface cues for direct stem cell differentiation.[12] In order to produce specific titanium nanotopography and attendant CaP surface chemistry properties a range of deposition techniques have been investigated including plasma spraying, pulse laser deposition (PLD), and radio frequency (RF) magnetron sputtering. RF magnetron sputtering, in particular, has been proven to be a particularly effective technique in this regard. Using appropriate titanium and hydroxyapatite sputter target materials provides for a Ti layer with a form of polycrystalline nanotopography and a CaP coating both as individual surfaces and in combination, that is, bioactive CaP on Ti nanotopography. By varying the deposition parameters, the interface between the substrate and the coating can be manipulated to provide the conditions necessary for direct MSC differentiation.[13] To date, most of the work in this area has focused on the application of RF magnetron sputtered Ti/CaP for control of the behavior of BMMSCs.[11] Hence, the utilisation of RF magnetron sputtered Ti/CaP surfaces to manipulate and understand PDLSC behavior is novel.

The central aim of this study is to examine the osteoblastic response of PDLSCs to three titanium test surfaces: an abraded titanium control surface (cpTi); a polycrystalline titanium surface, with both micro and nano-topography produced by radio frequency magnetron sputtering (TiTi); and the same surface incorporating a sputter deposited calcium phosphate coating (CaP-TiTi). In particular, the work reported here focuses on the delivery of surfaces with specific nanotopography and chemistry that have proven effectiveness for the direct (surface mediated) differentiation of stem cells. All of the surfaces produced were characterized in detail using Fourier transform infrared spectroscopy (FTIR), X-ray diffraction (XRD), X-ray photoelectron spectroscopy (XPS), and atomic force microscopy (AFM), in order to fully define the topography and surface chemistry created. The PDLSCs were cultured on the surfaces in the absence of any osteogenic supplement in the growth media. Osteoblastic responses were assessed for up to 21 days *in vitro* by measurement of real time q-PCR gene expression of alkaline phosphatase (ALPL), collagen type I alpha I (COL1A1), runt-related transcription factor (RUNX2), and secreted phosphoprotein 1 (SPP1). Additionally, Wnt signaling pathways were assessed by measuring gene expression for β-catenin (CTNNB1) and Wnt Family Member 5 A (WNT5A). Functional assessment of intracellular alkaline phosphatase (ALP) enzyme activity was also carried out. To the best of the authors' knowledge, this represents the first significant report of osteogenic differentiation of PDLSCs to these specifically defined surface cues in the absence of biochemical supplementation of media with osteogenic factors.

TABLE I. Nomenclature for the Surfaces Prepared for this Study

Sample Name	Nomenclature	Coating Thickness (nm)
Chemically pure titanium	cpTi	–
Titanium coated cpTi surfaces	TiTi	~100
Hydroxyapatite coated onto the TiTi surfaces	CaP-TiTi	~250

MATERIALS AND METHODS

Sample preparation

For this study 15 mm × 15 mm × 0.5 mm coupons of chemically pure titanium (cpTi), (Titanium International Ltd, UK) were abraded using a succession of 800, and 1200 grade SiC papers in order to prepare the surfaces to a consistent finish. The coupons were twice sonicated for 10 min each in acetone, isopropyl alcohol, and distilled deionized water. The abraded coupons were then dried thoroughly in a convection oven at 70°C for 12 h. From these samples, a range of different surfaces were prepared using RF magnetron sputtering. As detailed in Table I, the final sample types were abraded and cleaned chemically pure titanium surfaces (cpTi); polycrystalline titanium coated on the cpTi surfaces (TiTi); and calcium phosphate sputter coated onto the TiTi surfaces from a hydroxyapatite target (CaP-TiTi).

Sputtering procedure

For details of sputtering procedure see Supporting Information S1.

Characterization of the Ca-P powders and coatings

FTIR spectroscopy was carried out using a Varian 640-IR series instrument with a PIKE Diffuse Reflectance Infrared Fourier Transform Spectroscopy (DRIFTS) accessory. Samples were analysed in absorbance mode from 4000 to 400 cm^{-1} at a resolution of 4 cm^{-1} with 20 scans collected per sample. XRD was carried using a Bruker D8 Discover Diffractometer fitted with a Gobel Mirror. A Cu-Kα X-ray radiation ($\lambda = 1.540$ Å) source was employed with diffraction scans obtained at a tube voltage of 40 kV and a current of 40 mA. Scans were recorded from 20 to 50° 2θ with a step size of 0.04° and a dwell time of 30 s. For the grazing incidence angle XRD studies of CaP coatings on the cpTi

substrates the tube angle was set to 0.75°. XPS was carried out using a Kratos Axis Ultra DLD spectrometer. Spectra were recorded employing monochromated Al-Kα X-rays ($h\nu = 1486.6$ electron volts (eV)) with the anode operating at 10 kV and 15 mA (150 W). The base pressure was 1.33×10^{-7} Pa and the operating pressure was 6.66×10^{-7} Pa. A hybrid lens mode was employed during analysis (electrostatic and magnetic), with an analysis area of approximately 300 μm × 700 μm and a take-off angle (TOA) of 90° with respect to the sample surface normal. Wide energy survey scans (WESS) were obtained at a pass energy of 160 eV. High-resolution spectra were recorded for C1s, O1s, Ca2p, P2p, and Ti2p at a pass energy of 20 eV. The Kratos magnetic lens charge neutraliser system was used on all samples operating with a filament current of 1.95 to 2.00 A and a charge balance of between 3.3 and 3.5 V. Sample charging effects on the measured BE positions were further corrected by setting the lowest BE component of the C1s spectral envelope to 285.0 eV, that is, the value generally accepted for adventitious carbon surface contamination.[14] Photoelectron spectra were further processed by subtracting a linear background and using the peak area for the most intense spectral line of each of the detected elemental species to determine the % atomic concentration.

The surface topography was evaluated using a Digital Instruments Dimension 3000 Scanning Probe Microscope (SPM). The surface was scanned in tapping mode over 10 μm × 10 μm area using a force modulated etched silicon probe (FESP) with a nominal force constant of 0.28 N m^{-1}. A high frequency (75 kHz) z-oscillation was imposed upon the probe during *x*–*y* raster scanning, which provides for intermittent contact between the probe and the sample surface. This eliminates shear forces because the probe is not in constant contact with the sample. The images were collected as false color plots and subjected to minimal computational manipulation, allowing only for a tilt removal.

In vitro analysis

Explant procedure and isolation of periodontal ligament stem cells. Ethical approval was granted for the collection of teeth from the School of Dentistry, Belfast Health and Social Care Trust by the Office for Research Ethics Northern Ireland, (Approval Number 08/NIR03/15). See Supporting Information S2 for explant method and stem cell isolation.

Osteogenic gene expression of PDLSCs on test surfaces. To investigate the effect on osteoblastic gene expression from PDLSCs in contact with the various samples, cells were seeded in triplicate on each of the test surfaces at a density of 1×10^4/mL. At days 7, 14, and 21 coupons were carefully removed from their culture well and rinsed twice with cold phosphate-buffered saline. RNA was extracted using a RNeasy mini kit (Qiagen, UK) according to the manufacturer's instructions. RNA yield and purity was assessed on a Take3 plate (BioTek). Following this, cDNA was synthesized using the SuperScript vilo cDNA synthesis kit (Invitrogen, UK). The prepared cDNA was subsequently frozen (−80°C). Real-time qPCR for ALPL, COL1A1, RUNX2, and SPP1 was carried out on a Stratagene PCR machine (Agilent Technologies). Normalisation of results was achieved utilising the house-keeping genes Beta-2 microglobulin (B2M) and glucuronidase beta (GUSB) and deriving the geometric mean of these. Primer information is listed in Table II. Sequence amplification was performed as follows: denaturation at 55°C for 2 min and 95°C for 10 min followed by 45 cycles of 95°C for 30 s and 50°C for 1 min. The relative gene expression was calculated by the $2^{-\Delta\Delta CT}$ method. Results are reported as fold change of gene expression compared with the Ti surface (cpTi) at day 7, which was used in all experiments as the control value.

Wnt signaling pathway gene expression of PDLSCs on test surfaces. Similarly, to the protocol described in Osteogenic gene expression of PDLSCs on test surfaces section, real-time qPCR was used to investigate potential activation of Wnt signaling pathways by studying gene expression of CTNNB1 (canonical pathway) and WNT5A (noncanonical pathway). Primer information is listed in Table II. Gene expression was measured for the three test surfaces toward the later stages of differentiation on days 14 and 21. Normalisation of results was again achieved utilizing the house-keeping genes B2M and GUSB. Results are reported as fold change of gene expression compared with the cpTi surface at day 14.

Alkaline phosphatase (ALP) activity of PDLSC on test surfaces. To further assess the development of an osteoblastic phenotype from PDLSCs grown on the three test surfaces (cpTi, TiTi, CaP-TiTi), an ALP activity assay was performed on days 7, 14, and 21. Briefly, 1×10^4/mL PDLSCs were seeded in triplicate on each test surface. At each time point the coupons were carefully removed from their wells and put into a fresh 12-well plate, to avoid including cells growing around but not on the coupons. Surfaces were rinsed with PBS twice, and then lysed using 150 μL of lysis buffer (0.2% Triton X-100), followed by a 15 min incubation period at 37°C. The surfaces were then scraped to remove the lysed cells, which were then transferred to 1.5 mL tubes before vortexing and centrifugation at 4°C for 10 min. Supernatants were collected for quantification of ALP activity (Sigma-Aldrich, UK). ALP activity was normalized to total protein content, measured using a BCA protein assay kit (Pierce, Rockford, IL), and the results were expressed as ηmol PNPP/min/mg protein.

Statistical analysis. As indicated, all experiments were carried out in triplicate and results represent two independent experiments. Data points were analysed at 7, 14, and 21 days. One-way analysis of variance was used to determine statistical significance between gene expression for the samples and a Tukey *post hoc* test was used to determine significance between pairs of sample means. ALP activity data was analysed by the Kruskal-Wallis test for independent samples, followed by Dunn's test for multiple comparisons. The level of statistical significance was set at $p < 0.05$. The statistical analyses were performed with IBM SPSS Statistics for Windows (IBM Corp. Released 2012. Version 21.0. Armonk, NY).

TABLE II. qPCR Primer Information

Gene	Reference No.	Chromosome No.	Probe Sits on Exon Boundary	Base Position	Amplicon Length
COL1A1	Hs00164004_m1	17	1–2	230	66
RUNX2	Hs00231692_m1	6	5–6	900	116
			5–6	900	
			3–4	648	
ALPL	Hs01029144_m1	1	7–8	1056	79
			6–7	891	
			5–6	775	
SPP1	Hs00959010_m1	4	5–6	657	84
			6–7	699	
			5–6	618	
			4–5	576	
			7–8	888	
			4–5	1125	
CTNNB1	Hs00355045_m1	3	10–11	1948	86
			10–11	1962	
			10–11	1860	
			10–11	1922	
			10–11	1962	
WNT5A	Hs00998537_m1	3	4–5	748	61
			4–5	1343	
			4–5	703	
			7–8	6332	
			7–8	2956	
			4–5	849	
			4–5	1994	
			4–5	895	
			8–9	6059	
			7–8	2961	
B2M	HS00984230_m1	15	3–4	431	81
GUSB	HS00939627_m1	7	8–9	1522	96

RESULTS

Characterization of the Ca-P precursor powders

The HA target precursor powder was characterized using FTIR, XRD, and XPS to determine the nature of the material prior to sputter deposition of the CaP coatings used in this study. The results obtained were comparable to those described previously for similar HA powders.[15] From these findings it is clear that the purity, crystallinity and stoichiometry of the powder was as expected and confirmed the material was a carbonated from of HA.

Characterization of the surfaces

The FTIR spectrum for a CaP coating sputtered from HA target is shown in Figure 1. Well-resolved P-O stretching vibrations were observed as expected between 1100 and 950 cm^{-1}. O-P-O bending vibrations are also present between 620 and 560 cm^{-1}. Hydrogen phosphate bands (HPO_4^{2-}) can also be observed at 1122 and 582 cm^{-1}.[16] A very weak O-H libration band is observed around 632 cm^{-1} as a weak shoulder, with a further peak associated with O-H groups observed at 3570 cm^{-1}. This peak may be associated with O-H stretching groups within the film.[16] The absence of strong -OH functional groups, commonly observed at approximately 632 cm^{-1} and 3568 cm^{-1}, indicate that a degree of dehydroxylation has occurred within the CaP crystal structure deposited from the HA target under the conditions employed here. Peaks indicative of CO_3^{2-} species were also observed in the FTIR spectrum for Ca-P coating between 1550 and 1400 cm^{-1}.

The XRD pattern for the control substrate (cpTi) after abrasion was consistent with that observed for the International Centre for Diffraction Data (ICDD) file #44–1294 for titanium, as shown in Figure 2(a). The most intense peaks were observed at 35.3°, 38.5°, and 40.3° 2θ and relate to the 100, 002, and 110 reflections, respectively. The XRD

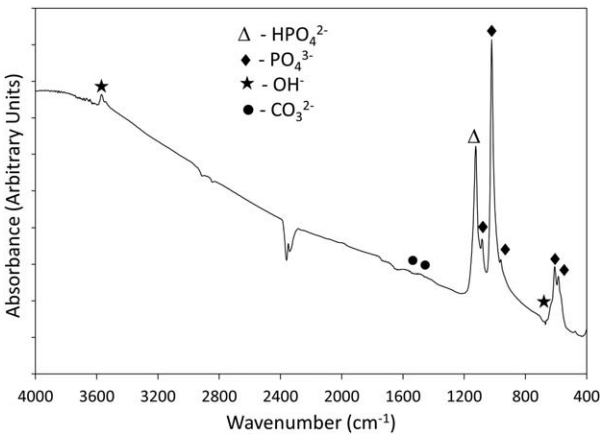

FIGURE 1. FTIR Spectrum for CaP-TiTi sample.

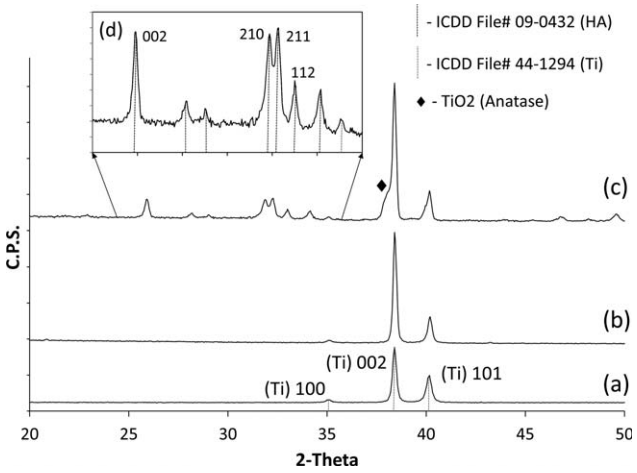

FIGURE 2. XRD diffractograms for (a) abraded chemically pure titanium surface (cpTi), (b) titanium layer sputtered onto a cpTi surface (TiTi), and (c and d) CaP coating on TiTi surface (CaP-TiTi).

pattern for the titanium layer sputter deposited onto the cpTi substrate (TiTi), as shown in Figure 2(b) had diffraction peaks in similar 2θ positions, however, this layer exhibits a clear 002 preferred orientation due to the relative intensity of the peak at 38.5° 2θ which dominates the diffraction pattern. The corresponding diffraction pattern for the CaP coating, as shown in Figure 2(c), has peaks that are clearly indicative of HA, with 2θ values that correspond closely to those observed in the ICDD file #09–0432 for HA. The four strongest peaks are observed at 25.9°, 31.7°, 32.1°, and 32.8° 2θ, and correspond to 002, 210, 211, and 112 reflections, respectively. The 002 reflection at 25.9° 2θ dominates the diffraction pattern, which suggests that this coating has a 002 preferred orientation as clearly observed in Figure 2(d). Peaks indicative of the underlying titanium layer are also present at 2θ values of 35.3°, 38.5° and 40.3° 2θ,[17] as per the ICDD file #44–1294 for titanium.

The XPS data are shown in Figures 3 to 5. For the cpTi surface after abrasion indicates the presence of oxygen, carbon and nitrogen in addition to titanium. The high-resolution Ti2p spectrum confirms the presence of TiO_2 due to the peaks at 458.6 eV ($Ti2p_{3/2}$) and 464.5 eV ($Ti2p_{1/2}$).[17,18] In addition, the peak observed at 453.5 eV ($Ti2p_{3/2}$) would normally be associated with metallic titanium.[18,19] The presence of a surface oxide layer is further confirmed by the nature of the high-resolution O1s spectral envelope, which clearly shows a strong contribution from TiO_2 at 530.4 eV. The contribution on the high B.E. side of the O1s peak at 530.4 eV may be a consequence of the presence of oxygen from organic species and/or OH groups.[17,18] Similar results were observed for the sputter deposited titanium layer (TiTi). However, in this case the contribution from the TiO_2 (459.0.0 eV ($Ti2p_{3/2}$) and at 464.7 eV ($Ti2p_{1/2}$)) is more dominant than that for the metallic state in the Ti2p high-resolution spectral envelope (which was not detected here). The XPS WESS and high-resolution scans for a CaP-TiTi surfaces, shows peaks corresponding to Ca2s (439.0 eV), $Ca2p_{3/2}$ (347.6 eV), $Ca2p_{1/2}$ (351.1 eV), Ca3s (44.3 eV), P2p (133.6 eV), P2s (190.9 eV), O1s (531.6 eV), and O_{KLL} Auger peak (978.0 eV). The key peak positions are highlighted in Table III and correspond closely to those reported for HA in the literature.[14] The Ca/P ratio for the CaP coating was 1.74 ± 0.14, as reported in Table IV, which is in close agreement with that expected for stoichiometric HA (1.67).

AFM analysis of the cpTi surface after abrasion indicates the presence of random abrasion scratches running across its surface. These features dominate the substrate surface and range in width from 0.5 to 2.0 μm. Small hillocks, pits and fissures, which vary in size up to 5.0 μm, are also seen regularly across the surface, particularly between the abrasion scratches, as shown in Figure 6(a). For TiTi surface, titanium crystallites of 0.39 ± 0.05 μm in diameter were observed across the surface and seem to have formed preferentially around the more prominent surface asperities on the substrate, as illustrated in Figure 6(b). These surface features were seen to range between 0.25 and 0.5 μm. It is also apparent that there has been significant in-filling of the larger pits and abrasion scratches on the substrate surface by the sputtered Ti layer as observed by a decrease in the surface roughness values when compared to those obtained for the control cpTi surface, as highlighted in Table V. The sputter deposited CaP coating on the TiTi surface exhibits more regular sized columnar features across the coating surface of diameter 0.32 ± 0.07 μm. These features were found to range from 0.2 to 0.43 μm in diameter. Again, the surface roughness for the CaP-TiTi surfaces was again seen to decrease with further apparent in-filling of the pits and abrasion scratches on the substrate surface.

In Vitro Results

Osteogenic gene expression analysis. The osteogenic phenotype of the PDLSCs following culture on each of the three surfaces was confirmed at the transcriptional level by genes encoding ALP, COL1A1, RUNX2, and SPP1. Figure 7 shows the fold change in gene expression for each gene relative to that for cpTi surface at day 7 which was used as a calibration value. For ALPL there was up-regulation for

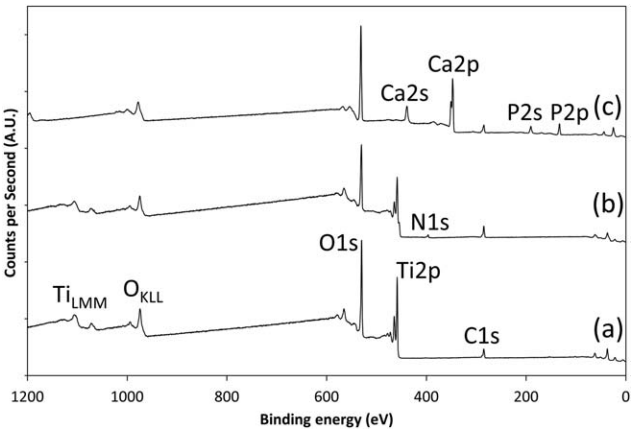

FIGURE 3. XPS wide energy survey scans (WESS) for (a) abraded chemically pure titanium surface (cpTi), (b) titanium layer sputtered onto a cpTi surface (TiTi), and (c) CaP coating on TiTi surface (CaP-TiTi).

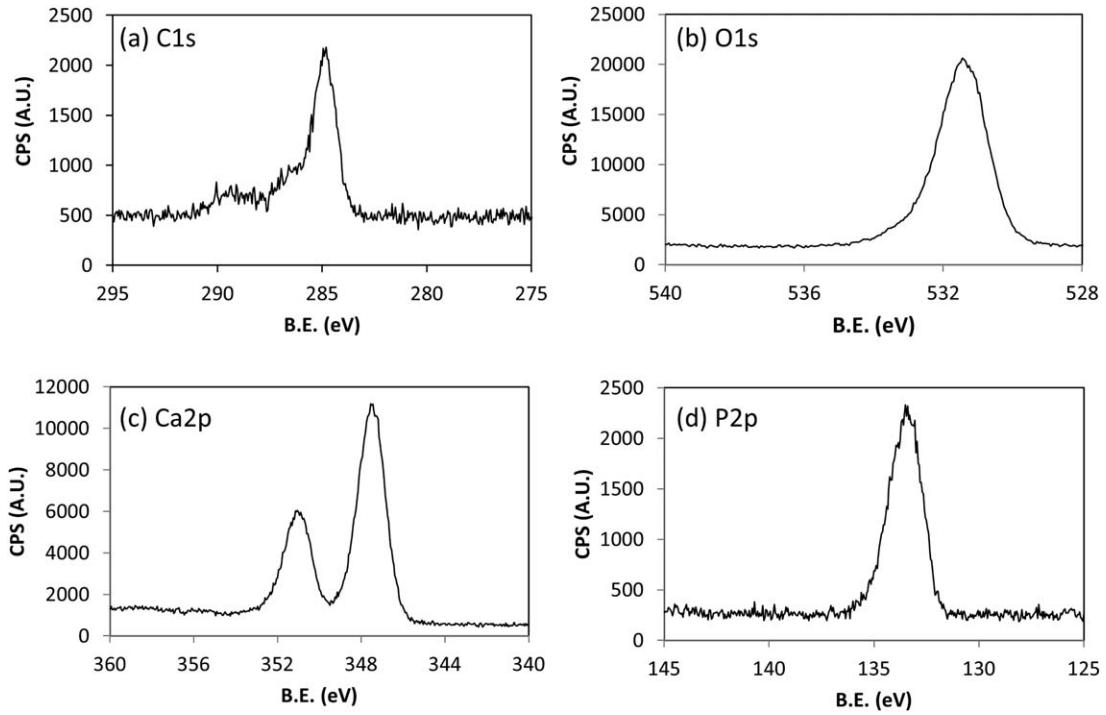

FIGURE 4. XPS high-resolution spectra for abraded titanium surface cpTi where (a) C1s, (b) O1s, and (c) Ti2p. Similar high resolution spectra for sputtered titanium surface (TiTi) are provided for (d) C1s, (e) O1s, and (f) Ti2p.

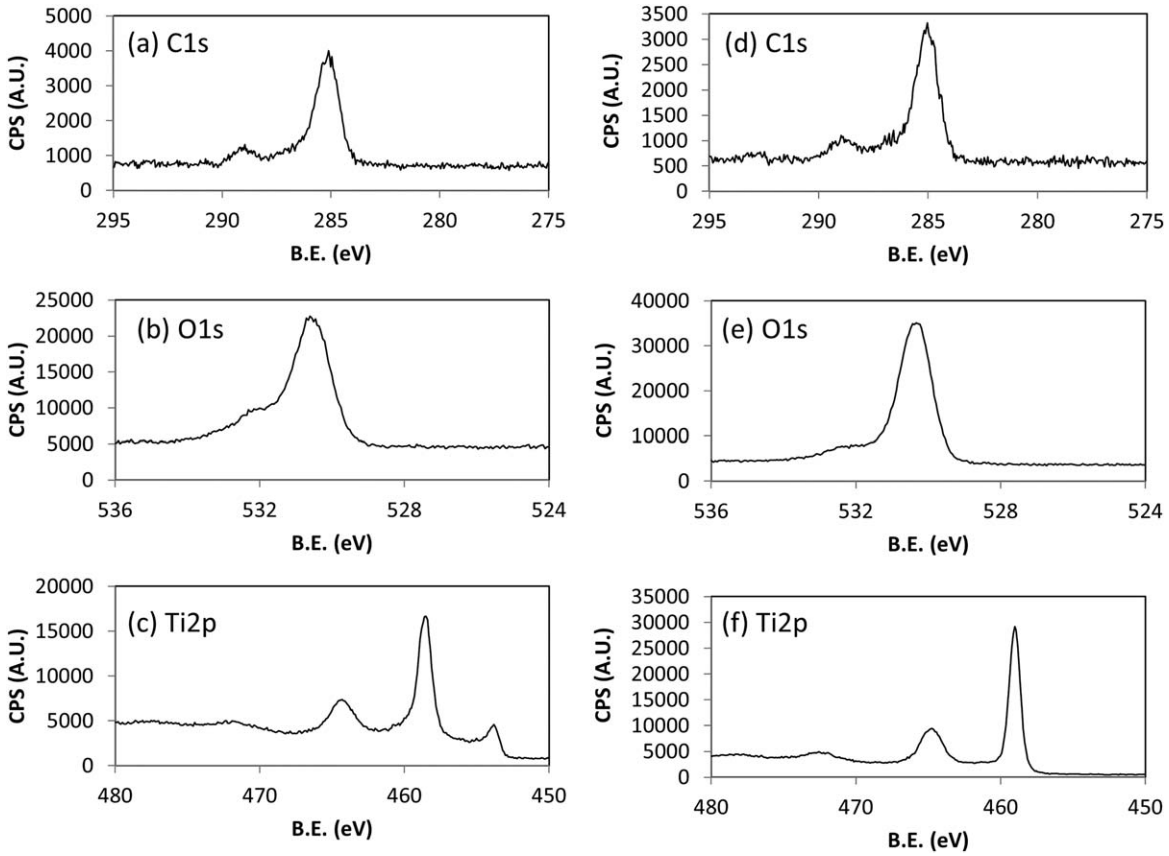

FIGURE 5. XPS high resolution spectra for the CaP-TiTi, where (a) C1s, (b) O1s, (c) Ca2p, and (d) P2p.

TABLE III. XPS Peak Position Data for the cpTi, TiTi, and CaP-TiTi Surfaces

	Peak Position (eV)					
Sample	C1s	O1s	$Ca2p_{3/2}$	P2p	$Ti2p_{3/2}$	N1s
cpTi	285.0	530.4	/	/	458.6	400.8
Ti on Ti	285.0	530.2	/	/	459.0	401.2
HA on Ti 500°C	285.0	531.6	347.6	133.6	/	/

PDLSCs cultured on both the cpTi surface and CaP-TiTi at day 14. This was followed by a significant down-regulation for the CaP-TiTi surface by day 21, whereas the cpTi surface continued to exhibit further up-regulation of ALPL. Despite the fact that the fold changes in gene expression were generally lower for COL1A, significant differences in expression were observed across all three time points. RUNX2 also displayed relatively low fold changes, with significant differences between the surfaces only seen at day 21. The largest fold change value was observed for the SPP1 gene, where there was a significant up regulation of x16.9 for the CaP-TiTi surface at day 21.

Wnt signaling pathways, gene expression. Wnt signaling was investigated at the transcriptional level by the genes encoding CTNNB1 for the canonical pathway, and WNT5A for the noncanonical pathway at days 14 and 21. Figure 8 shows the fold change in gene expression for each gene relative to that of the cpTi surface at day 14 which was used as a calibration value. A significant upregulation was observed for both CTNNB1 and WNT5A genes on the CaP-TiTi surface at days 14 and 21, respectively.

Alkaline phosphatase activity. At days 7 and 14 there was no significant difference between ALP activity on any of the three test surfaces compared to the control (Fig. 9). However, a significantly higher degree of ALP activity was observed for the CaP-TiTi surface by day 21 when compare to the cpTi and TiTi surfaces.

DISCUSSION

The differentiation of mesenchymal stem cells (MSCs) to various lineages can be modulated by a variety of signals including chemical cues, biomechanical cues, and biophysical cues. Studies investigating the influence of biophysical cues, specifically micro- and nanotopography, have demonstrated the robust role this effect has on dictating the cell fate.[19] Surfaces which incorporate both chemical and physical properties are of increasing interest as they offer the potential to engender responses for specific cell applications.[20] In this study we examined the response of PDLSCs to three test surfaces: an abraded titanium surface (cpTi) control; a polycrystalline titanium surface, with both micro and nano-topography produced by radio frequency magnetron sputtering (TiTi); and the same surface incorporating a sputter deposited calcium phosphate coating (CaP-TiTi).

The cpTi control surface is a physically abraded surface, which incorporates pits, fissures and hillocks with features that were up to 5.0 μm across as indicated by AFM analysis. XRD and XPS analysis confirmed that these surfaces were indeed pure titanium and contained no detectable impurities. The corresponding TiTi surface, which incorporated sputtered deposited polycrystalline titanium, had the effect of reducing the surface roughness, indicating that in-filling of the surface occurs as a consequence of the sputtering process. In addition, micro-crystallites of titanium in the range 0.25 to 0.5 μm across are visible right across the surface, particularly around surface asperities, where the surface energy will be lower. XPS showed that the TiO_2 contribution here is more dominant than that from the source metal. Low levels of nitrogen were also seen to be present on this surface. XRD highlights that the TiTi surface exhibits a clear 002 preferred orientation. These results suggest that although the TiTi surface is predominantly titanium, its surface chemistry and topography is different than that of the cpTi control material. The CaP-TiTi surface had a much reduced surface roughness compared to either the cpTi and TiTi samples. The microcrystallites seen for the TiTi surface again occur homogeneously across the entire sample confirming that the CaP coating conforms to the this polycrystalline topography.[21] It should also be noted that the CaP coatings were thermally annealed to 500°C, as coatings sputter deposited under the conditions employed here are typically amorphous in nature, and inherently physiologically unstable.[14] The chemistry of the sputtered CaP detected here reflects the low sputtering power employed (150 W), as such coatings have been shown to contain only HA-like properties with no other additional CaP phases or byproducts presence.[16] This means that this coating is consistent with the requirements of various international standards (ASTM 1185–03(2014), ASTM 1609–(08)2014, and ISO 13779 (Parts 2 and 3)). The Ca/P ratio of the CaP-TiTi sample was determined to be 1.74 ± 0.14, which is slightly higher than would be expected for pure hydroxyapatite (1.67). FTIR analysis highlighted that there had been hydrogenation of the phosphate functional groups in the Ca-P films with concurrent dihydroxylation. It is suggested that this has a significant influence on the atomic ordering in the CaP coating that is still inherent event after thermal annealing.[14] A significant reduction in OH^- groups means that the charge balance necessary within the crystal structure must therefore be provided by other means. HA (and CaP coatings) can undergo carbonate (CO_3^{2-}) substitution within the crystal lattice at multiples sites. Most notably, A-type

TABLE IV. XPS Quantitative Data for the cpTi, TiTi, and CaP-TiTi Surfaces

	Atomic Conc. %						Ca/P
Sample	C1s	O1s	Ca2p	P2p	Ti2p	N1s	Ratio
cpTi	25.7	48.1	/	/	26.2	/	/
TiTi	31.9	43.5	/	/	23.3	1.3	/
CaP-TiTi	18.1	55.8	15.6	10.4	/	/	1.74 ± 0.14

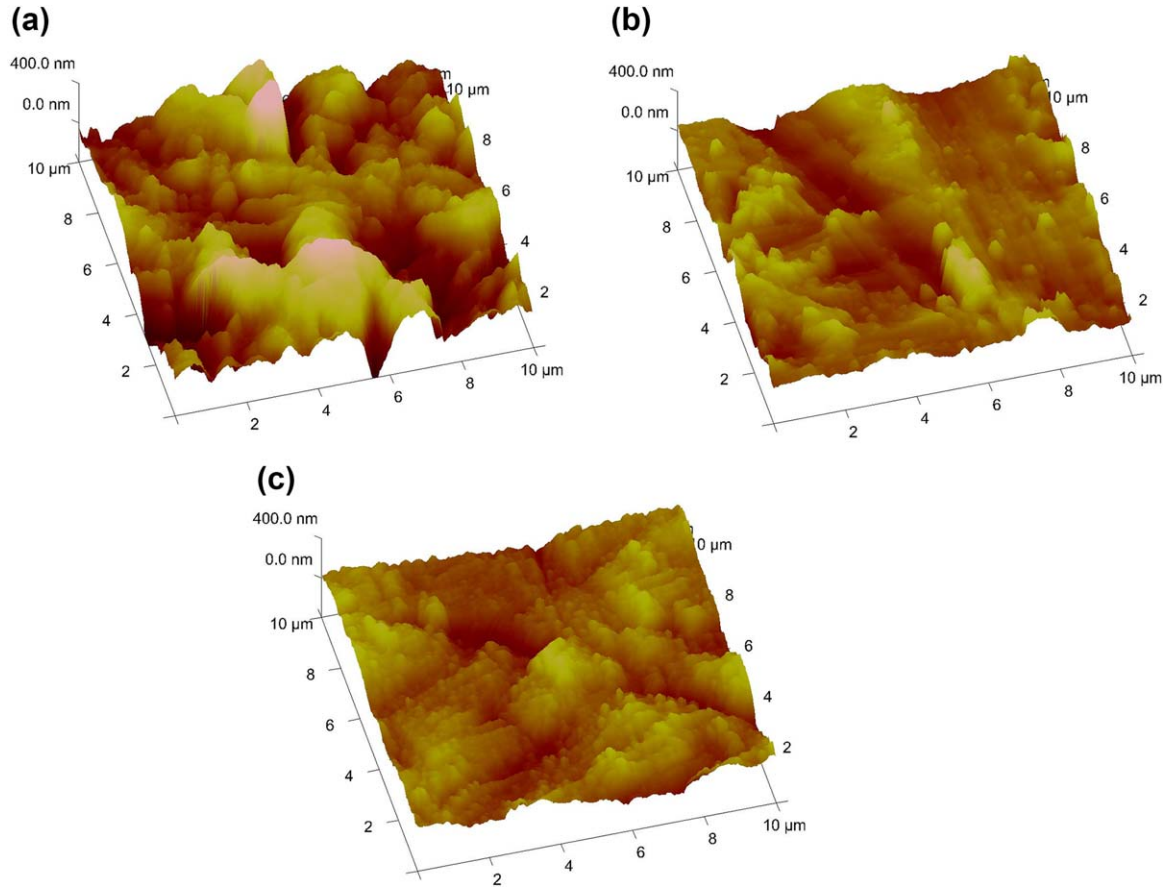

FIGURE 6. AFM images for (a) abraded titanium surface (cpTi), (b) titanium layer sputtered onto a cpTi surface (TiTi), and (c) CaP coating on TiTi surface (CaP-TiTi).

substitution for OH^- groups, B-type substitutions for PO_4^{3-} groups, or both (AB) substitution are acknowledged as providing for charge balance in the lattice structure of HA.[21,22] It is now widely accepted that in natural apatite, B-type substitutions dominate.[21] Evidence for some degree of CO_3^{2-} substitution here is suggested by the presence of these peaks between 1550 and 1400 cm^{-1} in the FTIR spectrum (Fig. 1). No evidence for the presence of CaO, $Ca(OH)_2$, or $CaCO_3$ was found in the XRD, FTIR, or XPS analyses. Therefore, the CaP coatings produced here can be said to resemble something close to naturally occurring apatite rather than synthetic HA in that they contain carbonate and are both dehydroxylated and non-stoichiometric.[23] Furthermore, it is assumed that the material deposited here is not a calcium deficient hydroxyapatite (CDHA) material $[Ca_{10\text{-}X}[(PO_4)_{6\text{-}X}(HPO_4)_X](OH)_{2\text{-}X}]$, as this would result in Ca/P ratio <1.67.[21] Furthermore, the presence of CO_3^{2-} is not seen in the CDHA system. The CO_3^{2-} and HPO_4^{2-} can occur either as substitutional ions in the lattice of the coatings obtained (or as labile materials), or both. The XRD results also show that the CaP-TiTi surface has a preferred 002 *c*-axis orientation. There is also a change in the relative peak intensities of the 211 and 112 peaks as would be expected for stoichiometric HA (Fig. 2(c,d)]. These observations are in line with previous studies on sputter deposited apatites.[18] Other work has also shown that a preferred 002 orientation in CaP coatings can enhance the cellular response *in vitro*,[13] in particular for MSCs.[24] It has also been reported that the bioactivity attributed to CaP materials originates due to the actions of free Ca^{2+} ions.[25] Based on these various observations, it is suggested that a possible formula for the coatings produced here is $Ca_{10\text{-}X\text{-}Y/2}[HPO_4)(PO_4)]_{6\text{-}X\text{-}Y}(CO_3)_Y(OH)_{2\text{-}X}$.[26] However, the possibility of labile CO_3^{2-} and HPO_4^{2-} occurring in the lattice of the CaP coating cannot be discounted.[27]

TABLE V. Surface Feature Size and Surface Roughness Values from AFM Analysis of cpTi, TiTi, and CaP-Titi

Sample Name	Surface Feature Size (µm)	R_a (µm)	R_q (µm)
cpTi	–	40.6 ± 9.0	49.6 ± 10.7
TiTi	0.39 ± 0.05	30.7 ± 9.1	39.1 ± 11.8
CaP-TiTi	0.32 ± 0.07	25.4 ± 5.2	31.5 ± 6.0

The biological analysis of PDLSCs cultured on the CaP-TiTi surface showed that this surface is capable of inducing osteogenic differentiation, as evidenced by both gene expression and ALP activity compared to the cpTi control. The osteogenic differentiation observed here is thus attributable to the attendant surface chemistry and topography.

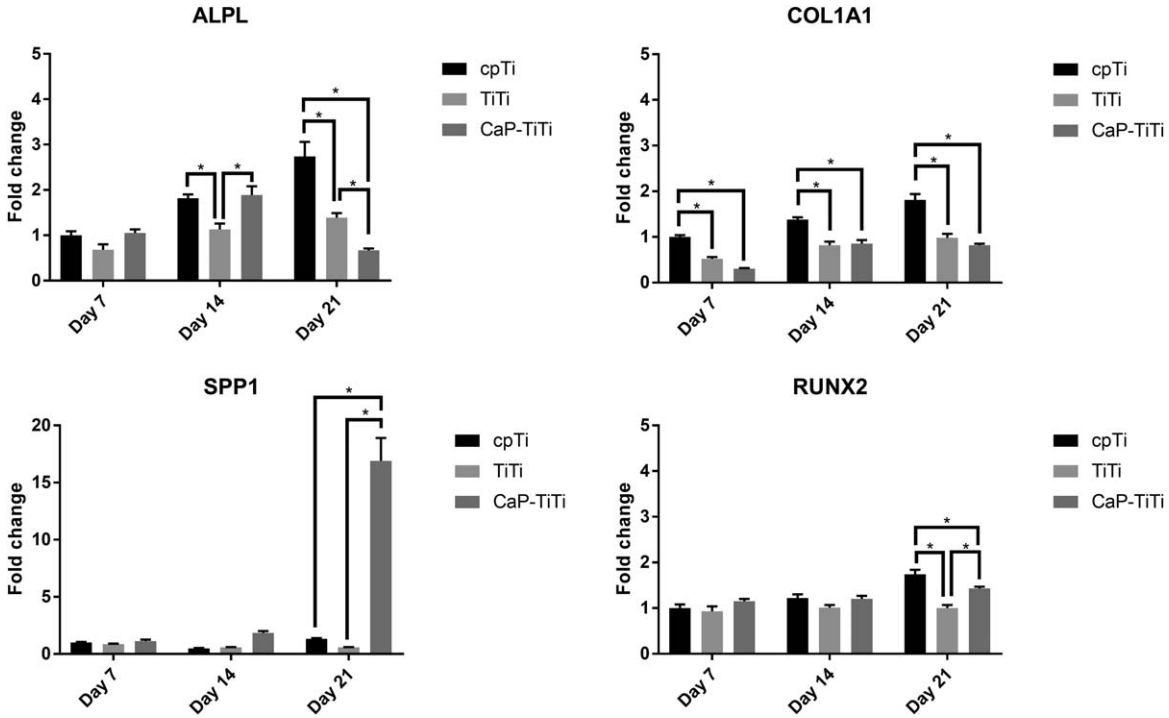

FIGURE 7. PDLSC bone-specific gene expression for ALPL, COL1A1, SPP1, and RUNX2. Levels provided as fold change relative to the day 7 cpTi surface. $*p < 0.05$ (ANOVA—post-test Tukey's).

The role of the CaP is clearly marked here by the fact there was little appreciable difference observed between the PDLSC response to TiTi surface and the cpTi, control. In this regard, the presence of titanium dioxide (TiO_2) which has been shown previously to enhance the osteoblast response of MSCs (compared to pure titanium surfaces),[28] was not apparent in the *in vitro* results obtained here. Moreover, given the similar surface features observed for the CaP-TiTi and TiTi surfaces, it would again suggest that the role of the CaP chemistry is the most significant factor in attaining an osteogenic response from the PDLSCs.

Undifferentiated mesenchymal stem cells tend to show weak alkaline phosphatase activity, whereas fully differentiated osteoblasts have higher activity. ALP may regulate the degradation of inorganic pyrophosphate providing sufficient local concentration of phosphate for mineralization.[29] Our results indicate that PDLSCs growing on the CaP-TiTi surface showed significantly higher ALP activity levels at day 21 compared to either the cpTi and TiTi surfaces. At the gene level, the ALPL gene codes for the production of alkaline phosphatase. The up regulation of alkaline phosphatase is generally regarded as an early marker of osteogenic differentiation. For example, Kulterer et al. observed that in the osteogenic differentiation of BMMSCs, up regulation of ALPL commenced on day 4, but by day 14 down regulation occurs as the cells start to enter the mineralization phase of phenotype change.[30] Similar behavior was observed in this study were up regulation of ALPL at day 14 was followed by a

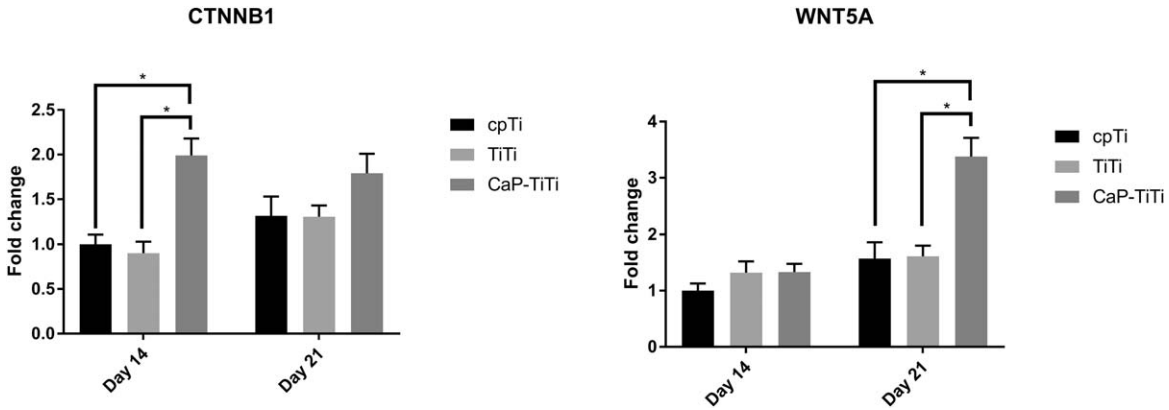

FIGURE 8. PDLSC Wnt pathway gene expression (a) CTNNB1 and (b) WNT5A at days 14 and 21. Levels provided as fold change relative to the day 14 cpTi surface. $*p < 0.05$ (ANOVA—post-test Tukey's).

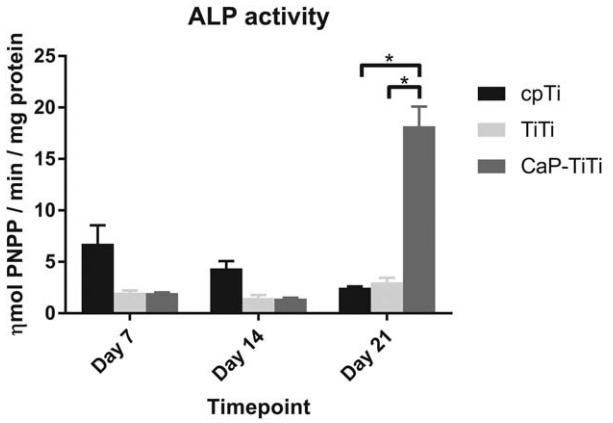

FIGURE 9. Alkaline phosphatase (ALP) activity for cpTi, TiTi, and CaP-TiTi surfaces at days 7, 14, and 21. Values were normalized to total protein content and expressed as mean ± SE ηmol PNPP/min/mg protein. *$p < 0.05$ (Kruskal-Wallis—post-test Dunn's).

significant down regulation at day 21 days for PDLSCs cultured on CaP-TiTi. By comparison, the cpTi control and TiTi surfaces showed up regulation at each time point. When these results are viewed in the context of the associated increase in functional ALP enzyme activity for PDLSCs seeded on the CaP-TiTi surface, it suggests that they are further along the osteogenic differentiation pathway by day 21.

The SPP1 gene (also known as Osteopontin or Bone Sialoprotein 1), codes for a secreted protein which binds hydroxyapatite with high affinity. It is generally considered a late marker of osteogenic differentiation, although its expression is known to peak twice: firstly around day 4 during proliferation and secondly between days 14 and 21 during mineralization.[31] In this study we observed a ×17-fold increase in the expression of SPP1 by day 21 for PDLSCs cultured on the CaP-TiTi surface. This again suggests that cells are entering a mineralisation stage of differentiation.

In addition to surface topographical cues, one of the important factors regulating cellular response is material solubility. This determines the type and concentration of dissolved ions in the cell environment. Previous work has shown that RF magnetron sputtering of hydroxyapatite onto titanium results in "as-deposited" coatings that are typically nonstoichiometric, with slightly Ca^{2+} rich surfaces.[17] Although the CaP surfaces here were thermally annealed to reduce their inherent solubility, it is still likely that some moderate dissolution occurs. This, in combination with the apparent 002 preferred orientation of the CaP coating produces a surface that is capable of releasing Ca^{2+} ions, known to play an important role in cell proliferation and differentiation, into the localized ECM/media.[32,33] Combining this with the micro- and nanoscale surface features that are produced by sputtering, offers a means for greater physical interaction between the cells and the CaP-TiTi surface.

RUNX2 is acknowledged as the central control gene within the osteoblast phenotype.[34] At early stage differentiation RUNX2 plays a major role in directing MSCs to the osteoblast lineage and triggering the expression of many extracellular bone matrix proteins.[35] At day 21 in this study there was only modest upregulations of ×1.7 and ×1.4-fold changes for the cpTi and the CaP-TiTi surfaces, respectively. Previous studies investigating RUNX2 expression have included an earlier time point, that is, at days 1, 3, or 4.[36−38] The inclusion of earlier time points in the present study may have provided a better baseline and more meaningful comparison of fold change analysis for RUNX2. Similarly, analysis of the COL1A1 expression showed only minor differences in fold changes. COL1A1 codes for production of type I collagen and plays an important role in cell adhesion, proliferation and differentiation of the osteoblast phenotype. It is considered to be an early marker of osteoprogenitor cells[39] and thus inclusion of an earlier time point for this gene may have allowed a more definitive conclusions to be drawn.

Previous work has shown that Wnt signaling through the canonical and non-canonical pathways modulate multiple aspects of osteoblast physiology including proliferation, differentiation, bone matrix formation, and apoptosis.[40] Significant upregulation was observed for both CTNNB1 and WNT5A genes on the CaP-TiTi surface at days 14 and 21 respectively. This would suggest the enhanced osteoblastic response of the CaP-TiTi surface is likely occurring through these Wnt signaling pathways (both canonical and noncanonical). This finding is in agreement with a previous study which showed modifying the physical and chemical properties of titanium surfaces could differentially effect the expression of osteo-modulatory molecules in PDLSCs grown on them.[5] By carefully characterizing surfaces using the RF sputtering technique in the present study, we for the first time were able to demonstrate that it is the additional chemistry of CaP on nanotopographic surfaces (CaP-TiTi) rather than nano-topographic features alone (TiTi) that is key in generating the direct osteoblastic differentiation of PDLCSs *in vitro*.

CONCLUSION

The CaP-TiTi surface directly promoted the osteogenic differentiation of PDLSCs in the absence of osteogenic inducing factors in the culture media. Differences in gene expression behavior associated with the osteogenic differentiation of the stem cells over a 21-day culture period were observed to be statistically significant on the CaP-TiTi surface when compared to both cpTi and TiTi samples. This was supported by *in vitro* analysis of ALP expression activity. Analysis of the CaP-TiTi surfaces indicate that it was comprised of a non-stoichiometric, carbonated, calcium rich (Ca/P ratio: 1.74) surface chemistry and that it is these properties which was likely to have been the key factors in driving the PDLSC down the osteoblastic differentiation pathway. Moreover, the data attained suggest that under the specific conditions applied, the topography present on the TiTi surface is not capable of directly providing an osteogenic response on its own. Hence, it has been shown here for the first time sputter deposited CaP coatings deposited on micro/nanoscale titanium topography can directly induce PDLSCs to an osteoblast cell lineage. These results support the promise of such surfaces for both the incorporation on dental device

surface and as a means to create osteogenic cells for enhanced implant fixation with appropriate *in vivo* studies now required to confirm this enhanced osteogenic and regenerative potential.

REFERENCES

1. Olivares-Navarrete R, Hyzy SL, Park JH, Dunn GR, Haithcock DA, Wasilewski CE, Boyan BD, Schwartz Z. Mediation of osteogenic differentiation of human mesenchymal stem cells on titanium surfaces by a Wnt-integrin feedback loop. Biomaterials 2011;32: 6399–6411.
2. Rausch-fan X, Qu Z, Wieland M, Matejka M, Schedle A. Differentiation and cytokine synthesis of human alveolar osteoblasts compared to osteoblast-like cells (MG63) in response to titanium surfaces. Dent Mater 2008 ;24:102–110. Jan
3. Seo BM, Miura M, Gronthos S, Bartold PM, Batouli S, Brahim J, Young M, Robey PG, Wang CY, Shi S. Investigation of multipotent postnatal stem cells from human periodontal ligament. Lancet 2004;364:149–155.
4. Heo YY, Um S, Kim SK, Park JM, Seo BM. Responses of periodontal ligament stem cells on various titanium surfaces. Oral Dis 2011;17:320–327.
5. Kim SY, Yoo JY, Ohe JY, Lee JW, Moon JH, Kwon YD, Heo JS. Differential expression of osteo-modulatory molecules in periodontal ligament stem cells in response to modified titanium surfaces. Biomed Res Int 2014;2014:452175.
6. Li X, Liao D, Gong P, Dong Y, Sun G. Biological behavior of neur2ally differentiated periodontal ligament stem cells on different titanium implant surfaces. J Biomed Mater Res A 2014;102:2805–2812.
7. Gao H, Li B, Zhao L, Jin Y. Influence of nanotopography on periodontal ligament stem cell functions and cell sheet based periodontal regeneration. Int J Nanomed 2015 ;10:4009–4027.
8. Albrektsson T, Johansson C. Osteoinduction, osteoconduction and osseointegration. Eur Spine J 2001;Suppl 2:S96–S101.
9. Olivares-Navarrete R, Hyzy SL, Hutton DL, Erdman CP, Wieland M, Boyan BD, Schwartz Z. Direct and indirect effects of microstructured titanium substrates on the induction of mesenchymal stem cell differentiation towards the osteoblast lineage. Biomaterials 2010;31:2728–2735. Apr
10. Sjöström T, Brydone AS, Meek RD, Dalby MJ, Su B, Mcnamara LE. Titanium nanofeaturing for enhanced bioactivity of implanted orthopedic and dental devices. Nanomedicine 2013;8:89–104.
11. McCafferty MM, Burke GA, Meenan BJ. Mesenchymal stem cell response to conformal sputter deposited calcium phosphate thin films on nanostructured titanium surfaces. J Biomed Mater Res A 2014;102:3585–3597.
12. Lobo SE, Glickman R, da Silva WN, Arinzeh TL, Kerkis I. Response of stem cells from different origins to biphasic calcium phosphate bioceramics. Cell Tissue Res 2015;361:477–495. Aug
13. Boyd AR, O'Kane C, O'Hare P, Burke GA, Meenan BJ. The influence of target stoichiometry on early cell adhesion of co-sputtered calcium-phosphate surfaces. J Mater Sci: Mater Med 2013;24:2845–2861.
14. Boyd AR, Meenan BJ, Leyland NS. Surface Characterization of the evolving nature of radio frequency (RF) magnetron sputter deposited calcium phosphate thin films after exposure to physiological solution. Surf Coat Technol 2006;200:6002–6013.
15. O'Kane C, Duffy H, Meenan BJ, Boyd AR. The influence of target stoichiometry on the surface properties of sputter deposited calcium phosphate thin films. Surf Coat Technol 2008;203:121–128.
16. Boyd AR, Rutledge L, Randolph LD, Mutreja I, Meenan BJ. The deposition of strontium-substituted hydroxyapatite coatings. J Mater Sci: Mater Med 2015;26:65.
17. Boyd AR, Duffy H, McCann R, Meenan BJ. Sputter deposition of calcium phosphate/titanium dioxide hybrid thin films. Mater Sci Eng C 2008;28:228–236.
18. Boyd AR, Burke GA, Duffy H, Cairns ML, O'Hare P, Meenan BJ. Characterization of calcium phosphate/titanium dioxide hybrid coatings. J Mater Sci: Mater Med 2008;19:485–498.
19. Zhao L, Liu L, Wu Z, Zhang Y, Chu PK. Effects of micropitted/nanotubular titania topographies on bone mesenchymal stem cell osteogenic differentiation. Biomaterials 2012 ;33:2629–2641. Mar
20. McCafferty MM, Burke GA, Meenan BJ. Mesenchymal stem cell response to conformal sputter deposited calcium phosphate thin films on nanostructured titanium surfaces. J Biomed Mater Res A 2014;102:3585–3597. Oct
21. Wopenka B, Pasteris JD. A mineralogical perspective on the apatite in bone. Mater Sci Eng C 2005;25:131–143.
22. Gibson IR, Bonfield W. Novel synthesis and characterization of an AB-type carbonate-substituted hydroxyapatite. J Biomed Mater Res 2002;59:697–708.
23. Vallet-Regí M, González-Calbet JM. Calcium phosphates as substitution of bone tissues. Prog Solid State Chem 2004;32:1–31.
24. Kim H, Camata RP, Chowdhury S, Vohra YK. In vitro dissolution and mechanical behavior of c-axis preferentially oriented hydroxyapatite thin films fabricated by pulsed laser deposition. Acta Biomater 2010;6:3234–3241. Aug
25. Geesink RG, de Groot K, Klein CP. Bonding of bone to apatite-coated implants. J Bone Joint Surg Br 1988;70:17–22.
26. Guo Y, Yao Y, Ning C, Guo Y, Chu L. Fabrication of mesoporous carbonated hydroxyapatite microspheres by hydrothermal method. Mater Lett 2011;65:2205–2208.
27. Magne D, Pilet P, Weiss P, Daculsi G. Fourier transform infrared microspectroscopic investigation of the maturation of nonstoichiometric apatites in mineralized tissues: A horse dentin study. Bone 2001;29:547–552. Dec
28. Wu J, Hayakawa S, Tsuru K, Osaka A. Low-temperature preparation of anatase and rutile layers on titanium substrates and their ability to induce in vitro apatite deposition. J Am Ceram Soc 2004;87:1635–1642.
29. Lovmand J, Justesen J, Foss M, Lauridsen RH, Lovmand M, Modin C, Besenbacher F, Pedersen FS, Duch M. The use of combinatorial topographical libraries for the screening of enhanced osteogenic expression and mineralization. Biomaterials 2009 ;30: 2015–2022. Apr
30. Kulterer B, Friedl G, Jandrositz A, Sanchez-Cabo F, Prokesch A, Paar C, Scheideler M, Windhager R, Preisegger KH, Trajanoski Z. Gene expression profiling of human mesenchymal stem cells derived from bone marrow during expansion and osteoblast differentiation. BMC Genomics 2007;8:70.
31. Aubin JE. Regulation of osteoblast formation and function. Rev Endocr Metab Disord 2001;2:81–94.
32. Dorozhkin SV. Surface reactions of apatite dissolution. J Colloid Interface Sci 1997;191:489–497.
33. Dorozhkin SV. A review on the dissolution models of calcium apatites. Prog Cryst Growth Charact Mater 2002;44:45–61.
34. Shui C, Spelsberg TC, Riggs BL, Khosla S. Changes in Runx2/Cbfa1 expression and activity during osteoblastic differentiation of human bone marrow stromal cells. J Bone Miner Res 2003;18: 213–221.
35. Komori T. Regulation of bone development and extracellular matrix protein genes by RUNX2. Cell Tissue Res 2010;339:189–195.
36. Oliveira NC, Moura CC, Zanetta-Barbosa D, Mendonca DB, Cooper L, Mendonca G, Dechichi P. Effects of titanium surface anodization with CaP incorporation on human osteoblastic response. Mater Sci Eng C Mater Biol Appl 2013;33:1958–1962.
37. Mendonca G, Mendonca DB, Simoes LG, Araujo AL, Leite ER, Duarte WR, Aragao FJ, Cooper LF. The effects of implant surface nanoscale features on osteoblast-specific gene expression. Biomaterials 2009;30:4053–4062.
38. Mendonca G, Mendonca DB, Aragao FJ, Cooper LF. The combination of micron and nanotopography by H(2)SO(4)/H(2)O(2) treatment and its effects on osteoblast-specific gene expression of hMSCs. J Biomed Mater Res A 2010;94:169–179.
39. Jikko A, Harris SE, Chen D, Mendrick DL, Damsky CH. Collagen integrin receptors regulate early osteoblast differentiation induced by BMP-2. J Bone Miner Res 1999;14:1075–1083.
40. Bodine PV, Komm BS. Wnt signaling and osteoblastogenesis. Rev Endocr Metab Disord 2006;7:33–39.